Design, Synthesis, and Biological Evaluation of Pyrrolo[2,1-*c*][1,4]benzodiazepine and Indole Conjugates as Anticancer Agents

Jeh-Jeng Wang,*,† Yu-Kai Shen,† Wan-Ping Hu,‡ Ming-Chu Hsieh,† Fu-Lung Lin,† Ming-Kuan Hsu,† and Mei-Hui Hsu†

Faculty of Medicinal and Applied Chemistry, and Faculty of Biotechnology, Kaohsiung Medical University, Kaohsiung City 807, Taiwan

Received September 26, 2005

A series of novel pyrrolo[2,1-*c*][1,4]benzodiazepine (PBD) hybrids linked with indole carboxylates is described. These compounds were prepared by linking C-8 of **3** (DC-81) with an indole 2-carbonyl moiety (**9**) through carbon chain linkers to afford PBD hybrid agents **17**−**21** in good yields. Preliminary in vivo tests show that these hybrid agents have potent antitumor activity. The cytotoxic studies of the hybrid agents on human melanoma A2058 cells indicate most of the hybrids induced higher cytotoxicity, better DNA-binding ability, an increase in the apoptotic sub-G1 population, and a significant reduction in $\Delta\Psi_{mt}$ relative to compound **3**. In addition, DNA flow cytometric analysis shows that hybrids actively induce a marked loss of cells from the G2/M phase of the cell cycle, which progresses to early apoptosis as detected by flow cytometry after double-staining with annexin V and propidium iodide (PI). Thus, we suggest that the hybrid agents are potent inducers of cell apoptosis in A2058 cells.

Introduction

Pyrrolo[2,1-*c*][1,4]benzodiazepines (**1**) (PBDs) are a group of potent, naturally occurring antitumor antibiotics produced by *Streptomyces* species.[1] The cytotoxic and antitumor effects of these compounds are believed to arise from modification of DNA, which leads to inhibition of nucleic acid synthesis and production of excision-dependent single- and double-strand breaks in cellular DNA.[2] These antibiotics have been proposed to covalently bond to N2 of guanine to form a neutral minor groove adduct.[3,4] Molecular modeling, solution NMR, fluorimetry, and DNA footprinting experiments reveal that the PBD monomers recognize three base pairs of DNA with an alkylating preference for 5′-AGA sequences.[1] **1** (tomaymycin), **2** (anthramycin), and **3** (DC-81); a PBD natural product from *Streptomyces roseiscleroticus*,[5] are the best known examples of the PBDs (Figure 1).[6] Although the natural occurring PBDs have potent anticancer activity they have been precluded from clinical application due to side effects.[7] Synthetic monoalalkylating analogues devoid of cardiotoxicity manifest relatively poor in vitro and in vivo potency. Recently, there has been increasing interest in the design and synthesis of DNA interstrand cross-linking as well as conjugate agents to enhance the sequence selectivity and increase selectivity for tumor cells.[8−13]

A template-directed approach studied by solution NMR and molecular modeling showed that two tomaymycin molecules can be covalently bound to a 10 mer duplex DNA, where the drug molecules are positioned on opposite strands six base pairs apart.[14] Further examination demonstrated that **4** (DSB-120, Figure 2),[8] a head-to-head linked tomaymycin dimer, generates a guanine−guanine interstrand cross-link on the same 10 mer, with drug−DNA adducts maintaining self-complementarity. However, an unusual conformation at the 8I nucleotide indicates that the five membered ring of **4** is more shallowly immersed in the minor groove, perhaps due to strained cross-linking with a very short linker unit.[15] Thurston and co-workers reported that DSB-120 and related synthetic analogues have promising in vitro cytotoxicity and interstrand DNA cross-linking activity.[8−10] An indole moiety incorporated into natural and synthetic anticancer agents such as **5** (CC-1065),[16] **6** (bizelesin),[17] **7** (UTA-6026),[18] and **8** (K-252a)[19,20] (Figure 2) shows potent cytotoxicity. These results encouraged us to design and synthesize a diversity of novel PBD conjugate agents.

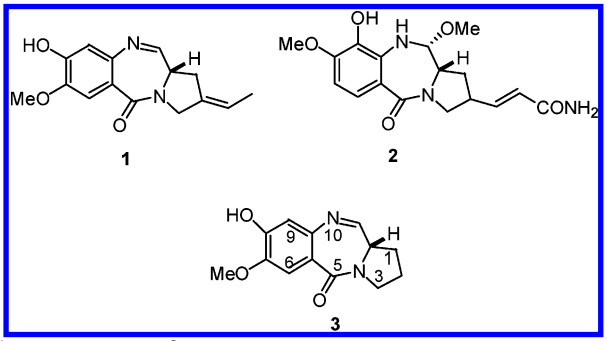

Figure 1. PBD analogues.

In the present study, we report the design, synthesis, and biological evaluation of a homologous series of PBD−indole conjugates.[21] The human melanoma cell line A2058 was selected as a model; it is a highly metastasizable cell line resistant to radio- and chemotherapy.[22] Meikrantz et al. reported the control of cell death is linked to the cell cycle.[23] Cells with a defective cell cycle are more vulnerable to some anticancer agents according to numerous preclinical studies. Many reports have indicated that mitochondria play a critical role in the commitment of cells to apoptosis.[24] Anticancer drugs may damage the mitochondria by increasing the permeability of the outer mitochondrial membrane, which is associated with collapse of mitochondrial membrane potential ($\Delta\Psi_{mt}$). Disruption in $\Delta\Psi_{mt}$ can be measured using rhodamine 123, a cationic lipophilic fluorochrome;[25] the extent of fluorescent dye uptake reflects the redox potential across the mitochondrial membrane.[26]

The aim of this study was to investigate whether hybrids possessed more cytotoxicity than **3**, and verify whether hybrid agents induced antiproliferation, leading to cell growth cycle perturbation, a decrease in $\Delta\Psi_{mt}$, and subsequent apoptotic cell death.

Results and Discussion

Chemistry. We prepared the indole-2-carbonyl moieties as shown in Scheme 1. Indole-2-carboxylic acid (**9**) was treated

* To whom correspondence should be addressed. Tel. (886)-7-312-1101 ext 2275, fax (886)-7-312-5339, e-mail: jjwang@kmu.edu.tw.
† Faculty of Medicinal and Applied Chemistry.
‡ Faculty of Biotechnology.

10.1021/jm050956q CCC: $33.50
Published on Web 01/26/2006

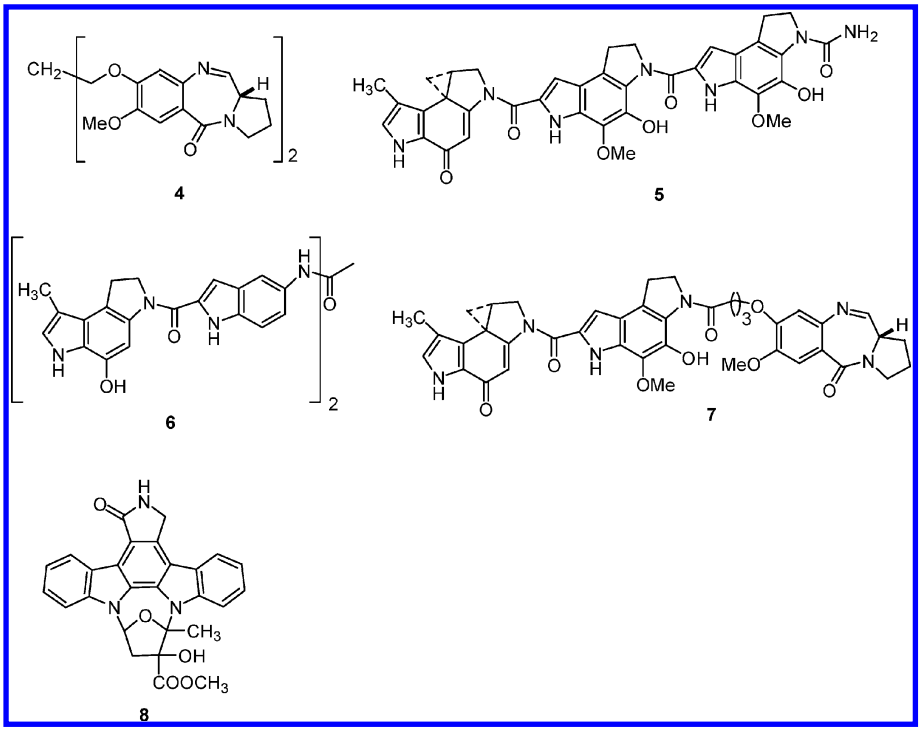

Figure 2. Antitimor agents.

Scheme 1. Synthesis of Indole-2-carbonyl Analogues **13**−**16**

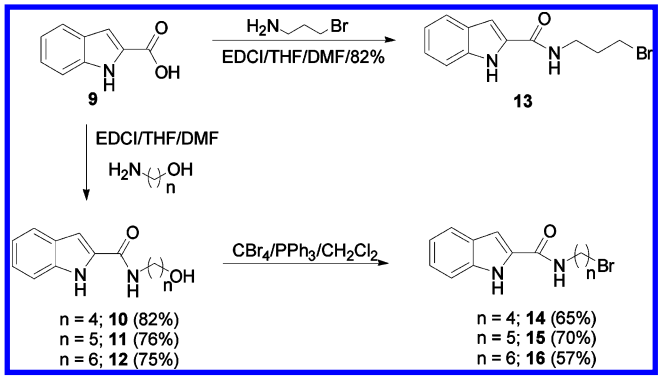

with commercially available 3-bromopropylamine ($n = 3$) in the presence of EDCI in dry THF and DMF at room temperature to afford *N*-(3-bromopropyl)-1*H*-2-indolecarboxamide (**13**) in 82% yield. The homologous analogues ($n = 4$ to 6) of indole-2-carbonyl **14**−**16** were prepared by bromination of hydroxyl compounds **10**−**12** with CBr_4 and PPh_3 in dry CH_2Cl_2. These hydroxyl compounds were obtained from condensation of indole-2-carboxylic acid with amine alcohols under standard EDCI coupling conditions in high yields. We have previously reported the efficient synthesis of **3** in excellent yield.[6,27] Reaction of **3** with **9** generated conjugate compound **17** in 75% yield (Scheme 2). Condensation of **3** with bromide compounds **13**−**16** in the presence of KI at room temperature afforded the desired homologous conjugate agents **18**−**21** in 60−70% yields (Scheme 2). This is the first example of the **3** molecule applied in this chemical reaction.

In Vitro Cytotoxic Effects. Conjugate agents **17**−**21** were assessed for their in vitro cytotoxicity on human melanoma cell line A2058. The activity of mitochondrial dehydrogenase enzymes, detectable by catalyzing MTS reagent, correlated with cell viability.[28] The cytotoxic effects of the six compounds **3**, and hybrid agents **17**−**21** on human melanoma cell line A2058 was examined using an MTS cell proliferation assay. The cell viability of A2058 cells treated with agents at different dosages

Scheme 2. Synthesis of PBD Conjugate Agents **17**−**21**

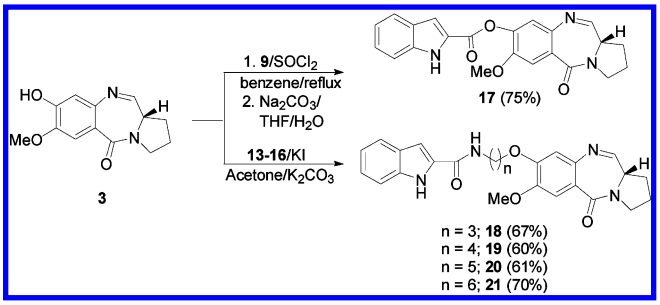

after 24 h is shown in Figure 3. The inhibitory effect is dependent on drug concentration. At concentrations larger than 3 μM, hybrid agents with the exception of **20** exhibited a higher inhibitory activity than **3** on A2058 cells.

The compounds **17** and **18** were selected by the US National Cancer Institute for evaluation in the in vitro preclinical antitumor screening program against 60 human tumor cell lines derived from nine cancer cell types. The selected biological

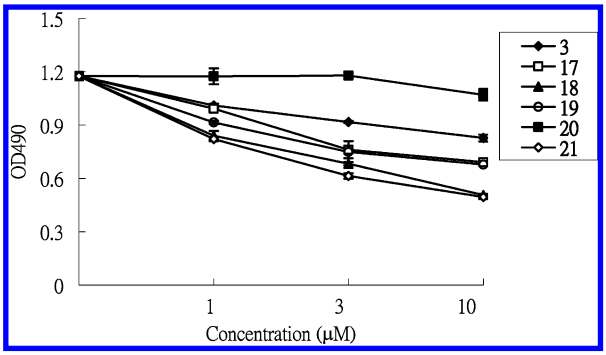

Figure 3. Dose−response curves for compounds tested against A2058 cells. Cells were seeded in a 96-well plate at 2500 cells per well and cultivated overnight until cell attachment. Compounds at the indicated concentration were added into the culture media in triplicate and incubated for 24 h before MTS being added. The conversion of MTS to formazan was measured at 490 nm. The absorbance is directly proportional to the number of living cells.

Table 1. In Vitro Cytotoxicity of Compounds **17** and **18** in Selected Cancer Cell Lines[a]

	GI_{50} (μM)	
panels/cancer cell lines	**17**	**18**
Non-Small Cell Lung Cancer		
EKVX	0.674	0.604
NCI-H522	0.198	0.0141
Colon Cancer		
COLO 205	0.196	0.118
HT29	0.185	0.274
CNS Cancer		
SF-268	0.669	0.027
U251	0.302	0.0394
Melanoma		
M14	0.162	0.173
UACC-62	0.290	0.203
Renal Cancer		
RXF 393	0.155	0.025
SN12C	0.21	0.41
Mean[b]	0.38	0.182

[a] Data obtained from NCI's in vitro disease-oriented tumor cells screen. [b] Mean values over 60 cell lines tested.

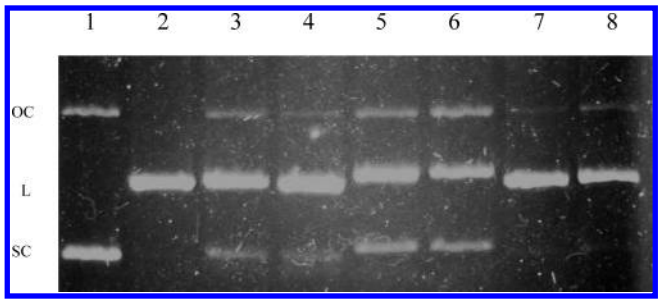

Figure 4. Agarose electrophoresis gel showing incubation of *BamH*I with complexes of pB*R*322, **3** and hybrid agents. Lane 1: control pB*R*322; lane 2: complete digest of pB*R*322 by *BamH*I; lane 3−8: agent-pB*R*322 complexes at 5 μM digested by *BamH*I were **3**, **17**, **18**, **19**, **20**, and **21**, respectively. (OC = open-circular, SC = supercoiled, L = linear).

evaluation results for the two compounds are presented in Table 1. The mean GI_{50} values for hybrid **17** and **18** are 0.38 and 0.182 μM, respectively, indicating that these agents have the potential for use as a highly potent broad-spectrum anticancer compound to inhibit the growth of a variety of cancer cell lines.[21]

In Vivo Cytotoxicity. Compounds **17** and **18** were further examined in an in vivo hollow fiber assay conducted by the National Cancer Institute, in which an intraperitonael (ip) sample and a subcutaneous (sc) sample were tested. In this assay, if a tested compound is observed to have a total of the ip plus sc scores larger than 20, it will be considered to be active and to have potential as an antitumor/anticancer drug candidate.[29] The preliminary in vivo testing results showed compounds **17** and **18** have total scores of 22 and 30, respectively. This indicates that they have potent antitumor/anticancer activity.

Enzyme Inhibition. The restriction endonuclease digestion assay is based on the ability of agent to inhibit the cleavage activity of restriction endonuclease *BamH*I.[30] The digestion assay gel includes two controls: open-circular (OC) and supercoiled (SC) pB*R*322 DNA in lane 1, and fully linearized DNA in lane 2. The experimental results show that hybrid agents (**18**, **19**, **21**) inhibit *BamH*I digestion (Figure 4). Our finding suggested that hybrid agents bind to DNA more efficiently than **3**.

Molecular Modeling Studies. To achieve monospecific binding GC,[31] we modified the 10-mer d(CGCGATCGCG)$_2$ in which the two G (guanine) underlined were each replaced with two I (inosine). Lacking the exocyclic 2-amino group, inosine is unreactive toward alkylation by **3**. The results obtained demonstrate that the hybrids **17**−**21** exhibit different DNA-binding activity (Table 2). It was found that hybrid **18**, **19**, and **21** form more stable complexes with DNA as compared to the other hybrids. The reason might be that the carbon chain linkers in the above hybrids form a better isohelical fit, giving rise to more favorable interaction within the minor groove than other hybrids. In addition, Baraldi et al.[32] mentioned that hydrogen bonds, electrostatic forces, and van der Waals interactions are responsible for the stability of the complex between these hybrid compounds and DNA. The binding of hybrid agents to double helix will be further studied.

Table 2. Energies (kcal/mol) of Covalent Complexes between Hybrid Compounds and d(CICGATCICG)$_2$

complex	energy (kcal/mol)
DNA−**17**	−329.3
DNA−**18**	−333.5
DNA−**19**	−331.4
DNA−**20**	−326.2
DNA−**21**	−331.1

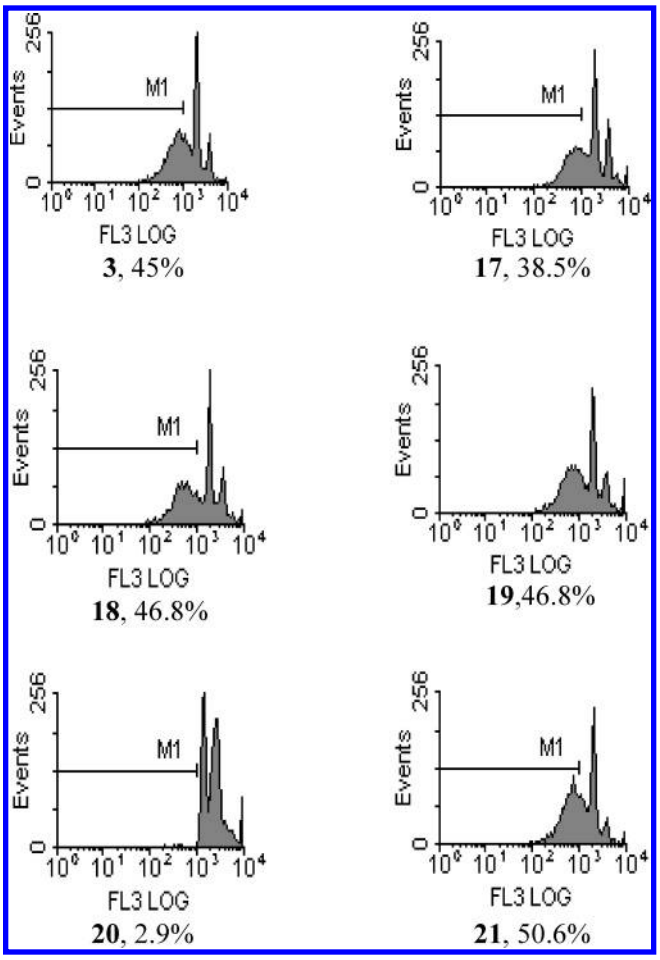

Figure 5. Effect of compound tested on the cellular sub-G1 content. A2058 cells were treated with 5 μM agents for 18 h and stained with PI. Cells were analyzed with the FACScan flow cytometer. Data represent the percentage of cell counts and display sub-G1.

Cell Cycle Effects. To investigate the effects of **3** and hybrids on cell cycle progression of A2058 cells, the DNA content of cell nuclei was measured by flow cytometric analysis. Agent action resulted in cells having a hypodiploid DNA content (sub-G1 material) that is characteristic of apoptosis and reflects fragmented DNA as shown in Figure 5. Treatment of A2058 cells with 5 μM agents for 18 h induced apoptosis effects in

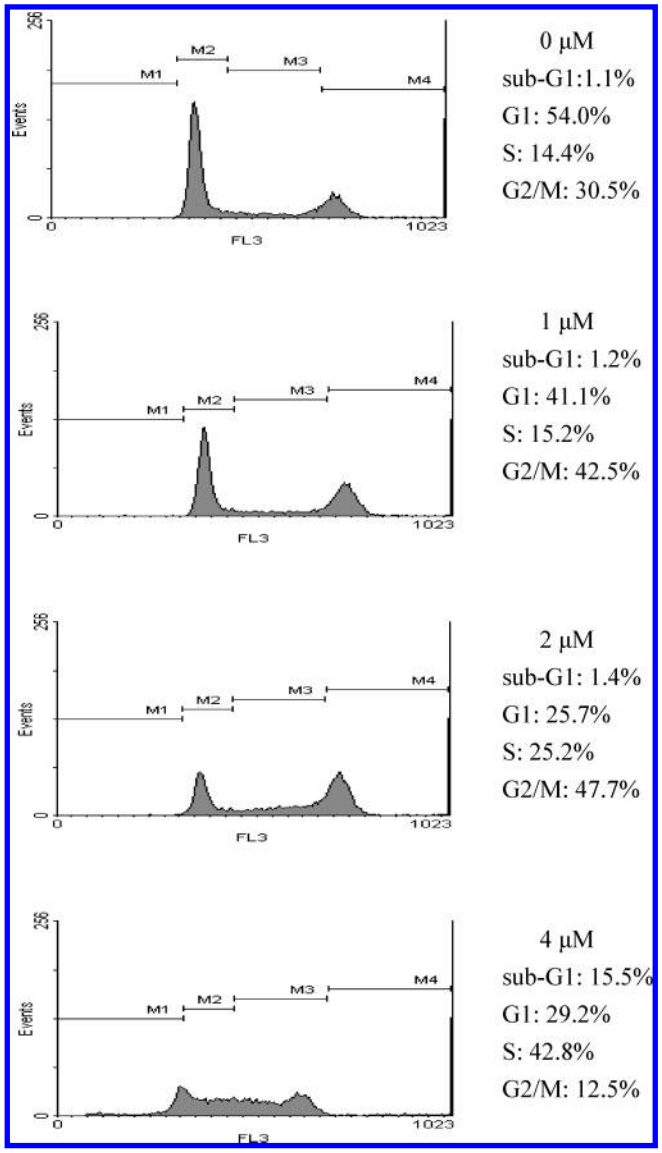

Figure 6. Flow cytometric analyses of cell cycle distribution of A2058 cells after exposure to hybrid **21** (0−4 μM) for 24 h before cell cycle analysis. M1 = apoptotic sub-G1 area; M2 = G1 area; M3 = S area; M4 = G2/M area.

45.0% (**3**), 38.5% (**17**), 46.8% (**18**), 46.8% (**19**), 2.9% (**20**), and 50.6% (**21**) of sub-G1 DNA peak. Our results show that hybrids **18**, **19**, and **21** were more efficient in inducing apoptosis than **3** in A2058 cells. Moreover, to verify whether cell damage might be attributable to the cell cycle program or might have become arrested at any cell cycle phases by hybrid-induced apoptosis in A2058 cells, we used hybrid **21** at various concentrations (Figure 6). The cells were treated with graded concentrations of the drug for 24 h. The majority of control cells exposed to DMSO of the cell cycle were in the G1 phase 54.0%, S phase 14.4%, and G2/M phase 30.5%. At a concentration of 2 μM, hybrid **21** treatment resulted in cells progressing to S and G2/M phases, while concomitantly the G1 population decreased. Furthermore, there is a marked loss of cells from the G2/M phase (from 47.7 to 12.5%) by hybrid **21** at a concentration of 4 μM. Our data indicate that hybrid **21** had cytotoxic effects on human melanoma A2058 cells, and the cytotoxic effects may be through apoptosis induction.

Mitochondrial Membrane Potential ($\Delta\Psi_{mt}$) Disruption. Previous studies have suggested that a decline of $\Delta\Psi_{mt}$ may be an early event in the process of cell death. Therefore, we

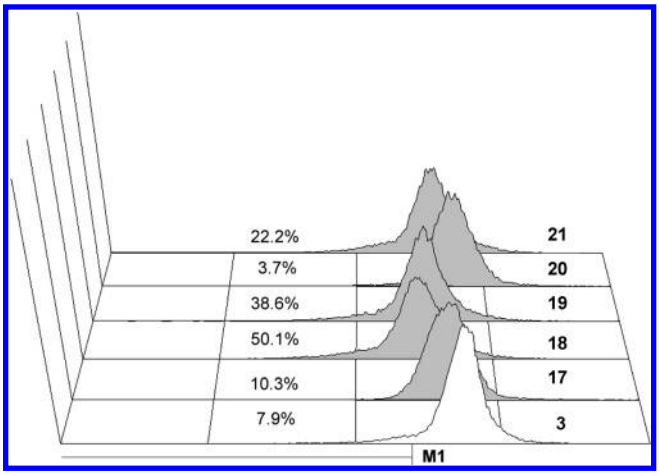

Figure 7. Effect of agent on the mitochondrial membrane potential ($\Delta\Psi_{mt}$). Cells were cultured with different agents at a concentration of 4 μM for 24 h and then stained with rhodamine 123 and analyzed immediately by flow cytometry as described under Materials and Methods. The number in M1 indicates the percentage of cells with reduced $\Delta\Psi_{mt}$.

investigated whether $\Delta\Psi_{mt}$ disruption was involved in agent-induced apoptosis. A2058 cells were treated with **3** and **17**−**21** at a concentration of 4 μM for 24 h and then analyzed by flow cytometry after rhodamine 123 dye labeling. The dye binds to the inner and outer membrane of mitochondria and undergoes a red shift in fluorescence during membrane depolarization.[33] The results are shown in Figure 7. Most hybrids exhibited a marked reduction in cellular uptake of the fluorochrome compared to **3**. The decrease of fluorescence intensity reflects the collapse of $\Delta\Psi_{mt}$, which generally defines an early but already inreversible stage of apoptosis.[34] These results reveal that exposure of melanoma A2058 cells to hybrids inducing the drop of $\Delta\Psi_{mt}$ may be a possible cause for the apoptotic process.

Apoptosis Detection. Fluorescein isothiocyanate (FITC)-conjugated annexin V has been utilized to detect the externalization of phosphatidylserine that occurs at an early stage of apoptosis propidium iodide (PI) is used as a marker of necrosis due to cell membrane destruction.[35] Although hybrids are highly potent antitumor agents, the precise mechanism of action remain unclear. To further characterize whether hybrid **21**-induced cell death involved apoptosis or not, we performed a biparametric cytofluorimetric analysis using annexin V and PI double staining. The distribution of stained cells is shown in Figure 8. A 2 μM concentration exhibited an apoptotic effect on A2058 cells, and higher concentrations induced cell death with increased cell permeability. The apoptotic effect was dependent on drug concentration.

Conclusions

We have previously reported an efficient synthesis of **3**, as a starting point for the design novel dimeric and conjugate agents that would be expected to be more biologically potent. We next combined **3** and an indole 2-carbonyl moiety to synthesize hybrids designed to have much higher sequence selectivity in DNA interactivity. NCI screening results indicate that these agents have the potential for use as highly potent broad-spectrum antitumor/anticancer compounds to inhibit the growth of a variety of cancer cell lines. Preliminary in vivo tests show that these hybrid agents have potent antitumor/anticancer activity. In further study, we used an MTS cell proliferation assay to evaluate the cytotoxicity of tested compounds in human

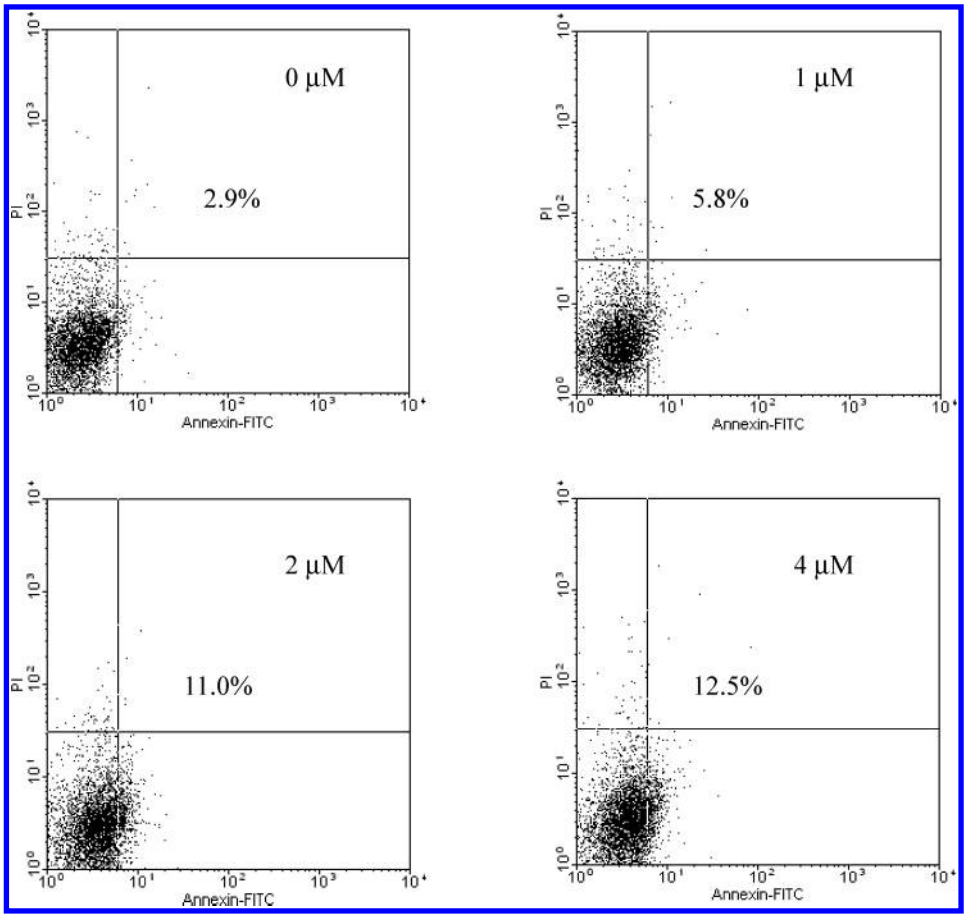

Figure 8. Hybrid **21** induces externalization of PS. Dot plots for A2058 cells treated with graded concentrations of **21** for 24 h and then stained with PI and an Annexin V-FITC conjugate specifically detecting the exposure of PS residues at the cell surface. For each drug concentration tested, the percentage of Annexin V^+ cells is given.

melanoma A2058 cells. Our results indicate that most of the hybrid agents are more effective as an antiproliferative agent than **3**. One can speculate that this is because hybrids recognize more DNA-binding sites and increase the stability of the drug/DNA complex. Thus, these compounds with DNA binding ability were further evaluated by restriction endonuclease *BamH*I and molecular modeling studies. The experimental results show that most of the hybrids inhibit *BamH*I digestion to a greater degree than **3**, and hybrids **18**, **19**, and **21** form more stable complexes with DNA as compared to the other hybrids. To identify whether the antiproliferative effect of hybrids were associated with cell cycle progression, hybrid **21** was selected against A2058 cells. The results obtained demonstrate that hybrid **21** induces a marked loss of cells from the G2/M phase and triggers apoptosis as revealed by the externalization of annexin V-targeted PS residues at the periphery of the cells. Owing to studies suggesting that a decline of $\Delta\Psi_{mt}$ may be an early event in the process of cell death, this prompted us to investigate whether $\Delta\Psi_{mt}$ disruption was involved in hybrid-induced apoptosis. In this study, most of the hybrids exhibited a marked reduction in $\Delta\Psi_{mt}$. Taken together, we provide evidence that hybrid agents are potent inducers of apoptosis in A2058 cells. We expect our studies can provide an important mechanistic insight into the action of hybrids.

Experimental Section

Synthetic Chemistry. Infrared spectra were recorded on a Perkin-Elmer Series 2000 spectrophotometer. ^{1}H NMR and ^{13}C NMR spectra were recorded at 400 and 100 MHz, respectively, using $CDCl_3$ as a solvent. ^{1}H NMR chemical shifts are referenced to TMS or $CDCl_3$ (7.26 ppm). ^{13}C NMR was referenced to $CDCl_3$ (77.0 ppm). Multiplicities were determined by the DEPT sequence as s, d, t, q. Mass spectra and high-resolution mass spectra (HRMS) were measured using the electron-impact (EI, 70 eV) technique by Taichung Regional Instrument Center of NSC at NCHU. Flash chromatography was carried out on Silica Gel 60 (E. Merck, 230−400 mesh).

The purity of the final compounds was analyzed with a Waters1525 Binary HPLC system connected to a Waters 2487 UV detector and following the peaks at λ= 221 nm. **Method A**: The flow was 1 mL/min and the gradient was from 70% acetonitrile-water, until 80% over a period of 10 min. The column for the analysis was Symmetry C18 (5 μm, 150 × 4.6 mm). **Method B**: The flow was 3 mL/min and the gradient was from 80% acetonitrile−water, until 90% over a period of 40 min. The column for the analysis was C18 of Hypersil ODS (5 μm, 250 × 21.2 mm).

General Procedure for the Syntheses of *N*2-(Alkanol)-1*H*-2-indolecarboxamides (10−12). To a stirred solution of indole-2-carboxylic acid (1 g, 6.2 mmol) and amino-1-alkanols (6.8 mmol) in THF (15 mL) and DMF (3 mL) was added EDCI (1.3 g, 6.8 mmol) in one portion under nitrogen at 0 °C. The resulting solution was stirred at room temperature for 24 h. The reaction mixture was poured into ice−water (150 mL) and extracted four times with ethyl acetate. The combined organic phases were washed with H_2O and brine and dried over $MgSO_4$. After removal of solvent, the residue was purified by flash chromatography (hexane/AcOEt = 5:1) to give the products.

***N*2-(4-Butanol)-1*H*-2-indolecarboxamide (10):** white solid; yield 1.10 g (82%); mp 141−143 °C. ^{1}H NMR ($CDCl_3$ + DMSO-d_6, 400 MHz) δ 10.68 (bs, 1H), 7.76 (bs, 1H), 7.61(d, J = 7.6 Hz, 1H), 7.45 (dd, J = 8, 0.8 Hz, 1H), 7.24 (dt, J = 8, 0.8 Hz, 1H), 7.08 (t, J = 7.6 Hz, 1H), 7.03 (d, J = 1.2 Hz, 1H), 3.65 (t, J = 6

Hz, 2H), 3.67−3.46 (m, 2H), 2.90 (bs, 1H), 1.79−1.63 (m, 4H); ^{13}C NMR ($CDCl_3$ + DMSO-d_6, 100 MHz) δ 161.3 (s), 136.0 (s), 131.2 (s), 127.0 (s), 123.2 (d), 121.1 (d), 119.5 (d), 111.6 (d), 102.4 (d), 61.3 (t), 38.9 (t), 29.5 (t), 25.8 (t); LRMS (EI, *m*/*z*) 232 (M+); HRMS (EI, *m*/*z*) for $C_{13}H_{16}N_2O_2$, calcd 232.1213, found 232.1209.

***N*2-(5-Pentanol)-1*H*-2-indolecarboxamide (11):** white solid; yield 1.17 g (76%); mp 120−122 °C. ^{1}H NMR ($CDCl_3$ + DMSO-d_6, 400 MHz) δ 10.68 (bs, 1H), 7.60 (d, J = 8 Hz, 1H), 7.52 (t, J = 6 Hz, 1H) 7.44 (dd, J = 6.0, 0.8 Hz, 1H), 7.22 (dt, J = 8.0, 1.2 Hz, 1H), 7.07 (dt, J = 8.0, 0.8 Hz, 1H), 7.04 (dd, J = 6.0, 0.8 Hz, 1H), 3.59 (t, J = 6.4 Hz, 2H), 3.45 (q, J = 6.8 Hz, 2H), 2.97 (bs, 1H), 1.68−1.41 (m, 6H); ^{13}C NMR ($CDCl_3$ + DMSO-d_6, 100 MHz) δ 161.6 (s), 136.3 (s), 131.1 (s), 127.1 (s), 123.5 (d), 121.3 (d), 119.7 (d), 111.8 (d), 102.8 (d), 61.6 (t), 39.2 (t), 31.9 (t), 28.9 (t), 22.9 (t); LRMS (EI, *m*/*z*) 246 (M+); HRMS (EI, *m*/*z*) for $C_{14}H_{18}N_2O_2$, calcd 246.1369, found 246.1372.

***N*2-(6-Hexanol)-1*H*-2-indolecarboxamide (12):** white solid; yield 1.15 g (75%); mp 120−122 °C. ^{1}H NMR ($CDCl_3$ + DMSO-d_6, 400 MHz) δ 10.72 (bs, 1H), 7.60 (d, J = 8 Hz, 1H), 7.49 (t, J = 5.6 Hz, 1H), 7.44 (d, J = 8 Hz, 1H), 7.22 (t, J = 8 Hz, 1H), 7.07 (t, J = 8 Hz, 1H), 7.04 (d, J = 2.4 Hz, 1H), 3.56 (t, J = 5.6 Hz, 1H), 3.44 (q, J = 6.8 Hz, 1H), 2.98 (bs, 1H), 1.62 (t, J = 6.8 Hz, 2H), 1.53 (t, J = 6.4 Hz, 2H), 1.41−1.36 (m, 4H); ^{13}C NMR ($CDCl_3$ + DMSO-d_6, 100 MHz) δ 161.6 (s), 136.3 (s), 131.1 (s), 127.2 (s), 123.5 (d), 121.3 (d), 119.7 (d), 111.8 (d), 102.8 (d), 61.7 (t), 39.2 (t), 32.2 (t), 29.2 (t), 26.3 (t), 25.1 (t); LRMS (FAB, *m*/*z*) 261 (M + H); HRMS (ESI, *m*/*z*) for $C_{15}H_{21}N_2O_2$ [(M + H)$^+$], calcd 261.1600, found 261.1603.

***N*2-(3-Bromopropyl)-1*H*-2-indolecarboxamide (13).** To a stirred solution of indole-2-carboxylic acid (100 mg, 0.62 mmol) and 3-bromoproppylamine (6.8 mmol) in THF (3 mL) and DMF (1 mL) was added EDCI (133.6 mg, 0.68 mmol) in one portion under nitrogen at 0 °C. The resulting solution was stirred at room temperature for 24 h. The reaction mixture was poured into ice−water (20 mL) and extracted four times with ethyl acetate. The combined organic phases were washed with H_2O and brine and dried over $MgSO_4$. After removal of solvent, the residue was purified by flash chromatography (hexane/AcOEt = 4:1) to give a light yellow solid **13**: yield 143.2 mg (82%); mp 101−103 °C. ^{1}H NMR ($CDCl_3$ + DMSO-d_6 400 MHz) δ 10.66 (s, 1H), 7.96 (s, 1H), 7.61 (d, 1H, J = 7.8 Hz), 7.46 (d, 1H, J = 7.4 Hz), 7.18−7.27 (m, 1H), 7.04−7.11 (m, 2H), 3.53−3.70 (m, 4H), 2.04−2.24 (m, 2H); ^{13}C NMR ($CDCl_3$ + DMSO-d_6, 100 MHz) δ 161.6, 135.1, 130.9, 127.0, 123.3, 121.2, 119.5, 111.6, 103.1, 37.4, 32.0, 30.9; LRMS (EI, *m*/*z*) 280 (M+); HRMS (EI, *m*/*z*) for $C_{12}H_{13}N_2OBr$, calcd 280.0212, found 280.0215.

General Procedure for the Syntheses of *N*2-(Bromoalkyl)-1*H*-2-indolecarboxamides (14−16). To a mixture of *N*2-(Alkanol)-1*H*-2-indolecarboxamides (1.94 mmol) and carbon tetrabromide (2.03 g, 5.82 mmol) in anhydrous dichloromethane (11 mL) was added, at 0 °C triphenylphosphine (1.03 g, 3.88 mmol). The resulting solution was stirred at room temperature for 3 h. After removal of solvent, the residue was purified by flash chromatography (hexane/AcOEt = 5:1) to give the products.

***N*2-(4-Bromobutyl)-1*H*-2-indolecarboxamide (14):** white solid; yield 371 mg (65%); mp 135−137 °C. ^{1}H NMR ($CDCl_3$ + DMSO-d_6, 400 MHz) δ 10.69 (bs, 1H), 7.75 (t, J = 5.6 Hz, 1H), 7.61 (dd, J = 8.4, 1.2 Hz, 1H,), 7.46 (dd, J = 8.4, 0.8 Hz, 1H), 7.22 (dt, J = 8.4, 1.2 Hz, 1H), 7.10−7.06 (m, 2H), 3.50−3.45 (m, 4H), 2.00−1.93 (m, 2H), 1.82−1.75 (m, 2H); ^{13}C NMR ($CDCl_3$ + DMSO-d_6, 100 MHz) δ 161.4 (s), 136.1 (s), 131.0 (s), 127.0 (s), 123.2 (d), 121.1 (d), 120.0 (d), 111.6 (d), 102.7 (d), 38.0 (t), 33.1 (t), 29.5 (t), 27.8 (t); LRMS (EI, *m*/*z*) 294 (M+); HRMS (EI, *m*/*z*) for $C_{13}H_{15}N_2OBr$, calcd 294.0369, found 294.0370.

***N*2-(5-Bromopentyl)-1*H*-2-indolecarboxamide hydrobromide (15):** light yellow solid; yield 527 mg (70%); mp 101−103 °C. ^{1}H NMR ($CDCl_3$ + DMSO-d_6, 400 MHz) δ 10.36 (bs, 1H), 7.63 (d, J = 7.6 Hz, 1H), 7.45 (dd, J = 8.0, 0.8 Hz, 1H), 7.33 (t, J = 5.6 Hz, 1H), 7.24 (dt, J = 8.0, 0.8 Hz, 1H), 7.10 (dt, J = 8.0, 0.8 Hz, 1H), 7.01 (d, J = 1.6 Hz, 1H), 3.49−3.40 (m, 4H), 1.94−1.87 (m, 2H), 1.70−1.63 (m, 2H), 1.57−1.50 (m, 2H); ^{13}C NMR ($CDCl_3$ + DMSO-d_6, 100 MHz) δ 161.7 (s), 136.3 (s), 131.1 (s), 127.3 (s), 123.7 (d), 121.5 (d), 120.0 (d), 111.8 (d), 102.7 (d), 39.1 (t), 33.5 (t), 32.0 (t), 28.6 (t), 25.2 (t); LRMS (EI, *m*/*z*) 388 (M + HBr); HRMS (EI, *m*/*z*) for $C_{14}H_{17}N_2OBr$+HBr, calcd 387.9786, found 387.9783.

***N*2-(6-Bromohexyl)-1*H*-2-indolecarboxamide (16):** white solid; yield 445 mg (57%); mp 118−120 °C. ^{1}H NMR ($CDCl_3$ 400 MHz) δ 9.85 (bs, 1H), 7.63 (dd, J = 8.0, 0.8 Hz, 1H), 7.45 (dd, J = 8.0, 0.8 Hz, 1H) 7.28 (dt, J = 8.0, 1.2 Hz, 1H), 7.13 (dt, J = 8.0, 0.8 Hz, 1H), 6.84 (d, J = 1.2 Hz, 1H), 6.29 (t, J = 5.6 Hz, 1H), 3.51 (t, J = 6.4 Hz, 2H), 3.39 (t, J = 6.4 Hz, 2H), 1.89−1.82 (m, 2H), 1.77 (s, HBr), 1.70−1.63 (m, 2H), 1.53−1.38 (m, 4H); ^{13}C NMR ($CDCl_3$, 100 MHz) δ 161.8 (s), 136.4 (s), 130.8 (s), 127.6 (s), 124.4 (d), 121.8 (d), 120.6 (d), 112.0 (d), 101.7 (d), 39.6 (t), 33.7 (t), 32.5 (t), 29.6 (t), 27.8 (t), 26.1 (t). LRMS (FAB, *m*/*z*) 323 [(M + H)$^+$]; HRMS (ESI, *m*/*z*) for $C_{15}H_{20}N_2OBr$ [(M + H)$^+$] calcd 323.0759, found 323.0760.

(11a*S*)-8-(1*H*-2-Indolecarbonyloxy)-7-methoxy-1,2,3,11a-tetrahydro-5*H*-pyrrolo[2,1-*c*][1,4]benzodiazepin-5-one (17). To a stirred solution of compound **3** (100 mg, 0.41 mmol) in THF (5 mL) and water (1 mL) was added $NaHCO_3$ (86 mg, 0.82 mmol) in one portion at 0 °C for 30 min. 1*H*-2-Indolecarbonyl chloride (118 mg, 1.12 mmol) in THF (5 mL), generated freshly by thionyl chloride, was added to the solution dropwise. The resulting solution was stirred at room temperature for 24 h. The reaction mixture was poured into ice water (30 mL) and extracted with ethyl acetate. The combined organic phases were washed with H_2O and brine dried over $MgSO_4$ and concentrated under vacuum. The crude product was subjected to flash chromatography (CH_2Cl_2/MeOH = 70:1) to give a white solid **17**: yield 119.6 mg (75%); mp 108−110 °C. ^{1}H NMR ($CDCl_3$, 400 MHz) δ 9.37 (s, 1H), 7.75−7.71 (m, 2H), 7.67 (s, 1H), 7.49−7.47 (m, 1H), 7.38 (dd, J = 6.8 and 1.2 Hz, 1H), 7.21−7.17 (m, 3H), 3.88−3.79 (m, 5H), 3.65−3.60 (m, 1H), 2.36−2.32 (m, 2H), 2.10−2.05 (m, 2H); ^{13}C NMR ($CDCl_3$, 100 MHz) δ 164.2 (s), 163.2 (d), 159.3 (s), 149.8 (s), 141.7 (s), 139.9 (s), 137.4 (s), 127.4 (s), 126.3 (s), 126.0 (d), 125.8 (s), 122.8 (d), 121.9 (d), 121.1 (d), 113.8 (d), 112.1 (d), 110.9 (d), 56.3 (q), 53.7(d), 46.8 (t), 29.6 (t), 24.1 (t); LRMS (FAB, *m*/*z*) 390 [(M + H)$^+$]; HRMS (FAB, *m*/*z*) for $C_{22}H_{20}N_3O_4$ [(M + H)$^+$] calcd 390.1455, Found 390.1445.

General Procedure for the Syntheses of (11a*S*)-8-[3-(1*H*-2-Indolycarboxamido)]alky-oxyl-7-methoxy-1,2,3,11a-tetrahydro-5*H*-pyrrolo[2,1-*c*][1,4]benzodiazepin-5-one (18−21). To a solution of **3** (100 mg, 0.41 mmol) in acetone (5 mL) was added K_2CO_3 (84 mg, 0.62 mmol) at 0 °C and stirred for 30 min. *N*2-(bromoalkyl)-1*H*-2-indolecarboxamides (**13**−**16**) 0.70 mmol, generated freshly in acetone (5 mL) and KI (41 mg, 0.60 mmol), was added to the solution dropwise. The resulting solution was stirred at room temperature for 24 h. The reaction mixture was poured into ice−water (30 mL) and extracted with ethyl acetate. The combined organic phases were washed with H_2O and brine dried over $MgSO_4$ and concentrated under vacuum. The residue was subjected to flash chromatography (CH_2Cl_2/MeOH = 40:1) to give products.

(11a*S*)-8-[3-(1*H*-2-Indolycarboxamido)]propoxyl-7-methoxy-1,2,3,11a-tetrahydro-5*H*-pyrrolo[2,1-*c*][1,4]benzodiazepin-5-one (18): white solid; yield 123 mg (67%); mp 106−108 °C. ^{1}H NMR ($CDCl_3$, 400 MHz) δ 9.59 (s, 1H), 7.67 (d, J = 4.4 Hz, 1H), 7.64 (dd, J = 0.8, 4.4 z, 1H), 7.57 (s,1H), 7.44 (dd, J = 8 and 0.8 Hz, 1H), 7.30−7.26 (m, 1H), 7.14 (dt, J = 7.2 and 1.2 Hz, 1H), 6.99 (dd, J = 2 and 0.8 Hz, 1H), 6.85 (s, 1H), 4.32−4.18 (m, 2H), 3.97 (s, 3H), 3.87−3.55 (m, 5H), 2.33−2.01 (m, 6H). ^{13}C NMR ($CDCl_3$, 100 MHz) δ 164.5 (s), 162.6 (d), 161.7 (s), 150.3 (s), 147.6 (s), 140.7 (s), 136.3 (s), 131.1 (s), 127.7 (s), 124.3 (d), 121.7 (d), 120.7 (d), 120.6 (s), 112.0 (d), 111.7 (d), 110.4 (d), 102.3 (d), 69.0 (t), 56.0 (q), 53.7 (d), 46.7 (t), 38.5 (t), 29.6(t), 28.6 (t), 24.2 (t); LRMS (FAB, *m*/*z*) 447 [(M + H)$^+$]; HRMS (FAB, *m*/*z*) for $C_{25}H_{26}N_4O_4$ [(M + H)$^+$] calcd 447.2034., Found 447.2028.

(11a*S*)-8-[3-(1*H*-2-Indolycarboxamido)]butoxyl-7-methoxy-1,2,3,11a-tetrahydro-5*H*-pyrrolo[2,1-*c*][1,4]benzodiazepin-5-one (19): white solid; yield 113 mg (60%); mp 114−116 °C. ^{1}H

NMR ($CDCl_3$, 400 MHz) δ 9.53 (bs, 1H), 7.67 (d, J = 4.4 Hz, 1H), 7.62 (dd, J = 8.0 and 0.8 Hz, 1H), 7.55 (s, 1H), 7.43 (dd, J = 8.0 and 0.8 Hz, 1H), 7.27 (dt, J = 8.0 and 1.2 Hz, 1H), 7.13 (dt, J = 8.0, 1.2 Hz, 1H), 7.02 (t, J = 6.4 Hz, 1H), 6.89 (d, J = 1.2 Hz, 1H), 6.83 (s,1H), 4.21−4.07 (m, 2H), 3.92 (s, 3H), 3.86−3.54 (m, 5H), 2.34−2.28 (m, 2H), 2.10−1.81 (m, 6H); ^{13}C NMR ($CDCl_3$, 100 MHz) δ164.6 (s), 162.6 (d), 161.7 (s), 150.4 (s), 147.6 (s), 140.7 (s), 136.2 (s), 131.0 (s), 127.7 (s), 124.3 (d), 121.8 (d), 120.5 (d), 120.3 (s), 111.9 (d), 111.5 (d), 110.2 (d), 101.9 (d), 68.7 (t), 56.1 (q), 53.7 (d), 46.7 (t), 38.7 (t), 29.6 (t), 26.6 (t), 25.6 (t), 24.2 (t); LRMS (FAB, *m*/*z*) 461 [(M + H)$^+$]; HRMS (FAB, *m*/*z*) for $C_{26}H_{29}N_4O_4$ [(M + H)$^+$] calcd 461.2191, Found 461.2190.

(11a*S*)-8-[3-(1*H*-2-Indolycarboxamido)]pentoxyl-7-methoxy-1,2,3,11a-tetrahydro-5*H*-pyrrolo[2,1-*c*][1,4]benzodiazepin-5-one (20): white solid; yield 119 mg (61%); mp 101−103 °C. ^{1}H NMR ($CDCl_3$, 400 MHz) δ 9.62 (bs, 1H, NH), 7.67 (d, J = 3.6 Hz, 1H), 7.62 (d, J = 8 Hz, 1H), 7.51 (s, 1H), 7.43 (dd, J = 8.0 and 0.8 Hz, 1H), 7.26 (dt, J = 8.0 and 0.8 Hz, 1H), 7.12 (dt, J = 7.6 and 0.8 Hz, 1H), 6.86 (d, J = 2.8 Hz, 1H), 6.81 (s,1H), 6.57 (t, J = 6.0 Hz, NH), 4.12−4.00 (m, 2H), 3.88 (s, 3H), 3.85−3.50 (m, 5H), 2.34−1.54 (m, 10 H); ^{13}C NMR ($CDCl_3$, 100 MHz): δ 164.7 (s), 162.4 (d), 161.7 (s), 150.8 (s), 147.7 (s), 140.6 (s), 136.2 (s), 130.9 (s), 127.6 (s), 124.3 (d), 121.8 (d), 120.5 (d), 120.1 (s), 111.9 (d), 111.6 (d), 110.4 (d), 101.9 (d), 68.8 (t), 56.1 (q), 53.7 (d), 46.7 (t), 39.5 (t), 29.6 (t), 29.2 (t), 28.4 (t) 24.2 (t), 23.5 (t). LRMS (FAB, *m*/*z*) 475 [(M + H)$^+$]; HRMS (FAB, *m*/*z*) for $C_{27}H_{30}N_4O_4$ [(M + H)$^+$] calcd 475.22347, Found 475.2353.

(11a*S*)-8-[3-(1*H*-2-Indolycarboxamido)]hexoxyl-7-methoxy-1,2,3,11a-tetrahydro-5*H*-pyrrolo[2,1-*c*][1,4]benzodiazepin-5-one (21): white solid; yield 140 mg (70%); mp 104−106 °C. ^{1}H NMR ($CDCl_3$, 400 MHz) δ 9.69 (bs, 1H), 7.67 (d, J = 4.0 Hz, 1H), 7.63 (d, J = 7.6 Hz, 1H), 7.52 (s, 1H), 7.42 (dd, J = 8.0 and 0.8 Hz, 1H), 7.27 (dt, J = 8.0 and 0.8 Hz, 1H), 7.12 (dt, J = 7.6 and 0.8 Hz, 1H), 6.86 (d, J = 1.6 Hz, 1H), 6.83 (s,1H), 6.46 (t, J = 5.6 Hz, 1H), 4.14−4.00 (m, 2H), 3.92 (s, 3H), 3.85−3.45 (m, 5H), 2.34−2.28 (m, 2H), 2.09−1.96 (m, 2H), 1.90−1.42 (m, 8H); ^{13}C NMR ($CDCl_3$, 100 MHz) δ 164.7 (s), 162.4 (d), 161.7 (s), 150.8 (s), 147.8 (s), 140.6 (s), 136.3 (s), 130.9 (s), 127.6 (s), 124.3 (d), 121.8 (d), 120.5 (d), 120.0 (s), 112.0 (d), 111.5 (d), 110.4 (d), 101.9 (d), 68.8 (t), 56.1 (q), 53.7 (d), 46.7 (t), 39.5 (t), 29.7 (t), 29.6 (t), 28.6 (t), 26.5 (t), 25.5 (t), 24.2 (t); LRMS (FAB, *m*/*z*) 489 [(M + H)$^+$]; HRMS (FAB, *m*/*z*) for $C_{28}H_{32}N_4O_4$ [(M + H)$^+$] calcd 489.2504, Found 489.2511.

Cell Culture. Human melanoma A2058 cells purchased from American Type Culture Collection (Manassas, VA) were maintained in Dulbecco's minimal essential medium (DMEM) supplemented with 10% FCS and 100 U/mL penicillin G and 100 μg/mL streptomycin sulfate (Gibco, BRL). A2058 cells were passaged at confluence after treatment with 5 mM EDTA (Gibco, BRL) and incubated at 37 °C in a humidified atmosphere containing 5% CO_2.

MTS Cell Proliferation Assay. A commercially available kit (CellTiter96 Aqueous proliferation assay kit, Promega, Madison, WI) was used to detect the proliferation according to the manufacturer's instruction. Cells were seeded in a 96-well plate at the cell density of 2500 cells/well. After an overnight incubation, the cells were treated with **3** or hybrid **17**−**21** at 5 μM and incubated for 24 h. The MTS reagent contains tetrazolium salt, [3-(4,5-dimethylthiazol-2-y1)-5-(3-carboxymethoxyphenyl)-2-(4-sulfophenyl)-2*H*-tetrazolium], premixed with the electron coupling reagent (phenazine ethosulfate) and was added into each well in 20 μL portions. The plate was then incubated for 1−2 h at 37 °C. The optical density value was detected by a microplate reader (MRX-II, Dynex technology, Chantilly, VA), whose detecting and reference wavelengths were set at 490 and 690 nm, respectively.

Restriction Endonuclease Digestion Assay. Compound−DNA complexes were prepared by incubating plasmid DNA (0.5 μg) with compound at 5 μM in restriction buffer (pH 7.5) and bovine serum albumin (BSA) (0.1 mg/mL) in a reaction volume of 19 μl at 37 °C for 1 h. An excess of *BamH*I (20 units in 1 μL) was added and incubated at 37 °C for a further 1 h. Each digestion was stopped by incubation at 65 °C for 20 min followed by lowering the temperature at 4 °C for 10 min. Then 20 μL (150 ng of plasmid DNA) from each digestion was added to 4 μL of loading buffer and loaded onto a 1.0% horizontal agarose gel which was run in Tris-acetate EDTA buffer (TAE−40 mM Tris base, pH 8.0, 18 mM glacial acetic acid, 1 mM EDTA) at 100 V for 2 h. The gels were stained with ethidium bromide (2 μg/mL) for 30 min and then destained in TAE buffer for 10 min. The DNA bands were visualized by UV and photography.

Molecular Modeling Studies. All of the calculations described below were performed using INSIGHT II suite of software (MSI, Inc.) running on a Silicon Graphics O_2 system.

1. Molecular Mechanics (MM) Calculations. The model of d(CICGATCICG)$_2$ and hybrid compounds were constructed using the BIOPOLYMER and BUILDER module, respectively. Docking of a hybrid compound into the minor groove of the DNA duplex was carried out manually and formed a covalent bond between C11 of the drug and a single reactive guanine (G4) on one strand of d(CICGATCICG)$_2$. The potentials and the charges were fixed using the AMBER force field.[36] The complex was minimized using steepest descent and conjugate gradient techniques until the energy root-mean-square gradient was less than 0.1 kcal/molÅ.

2. Molecular Dynamics (MD) Simulations. The minimized models were then subjected to 100 ps of molecular dynamics at 300 K with a gradual increase in temperature from 10 to 300 K over the first 10 ps. During simulations, all of the intermittent structures of the complexes formed at every successive 5 ps were saved and later they were subjected to energy reminimization to <0.1 kcal/molÅ.

Cell Cycle Analysis. A2058 cells were treated with compounds at 5 μM for 18 h or treated with various concentrations (0−4 μM) of hybrid **21** for 24 h. Cells were harvested by trypsinization and centrifugation. After being washed with PBS, the cells were fixed with ice-cold 70% ethanol for 30 min, washed with PBS, and then treated with 1 mg/mL of RNase A solution (containing 0.112 mg/mL of trisodium citrate) at 37 °C for 30 min. Cells were harvested by centrifugation at 400*g* for 5 min and further stained with 250 μL of DNA staining solution (10 mg of propidium iodide (PI), 0.1 mg of trisodium citrate, and 0.03 mL of Triton X-100 were dissolved in 100 mL of H_2O) at room temperature for 30 min in the dark. After loading 750 μL of PBS, the DNA contents of 10 000 events were measured by FACSscan flow cytometer (Elite ESP, Beckman Coulter, Brea, CA). Histograms were analyzed using Windows Multiple Document interface software (WinMDI).

Assessment of Mitochondrial Membrane Potential (ΔY_{mt}). A2058 cells were cultured in six-well plates and allowed to reach exponential growth for 24 h before treatment. The cells were harvested 24 h after treatment with compound (**3**, hybrid **17**−**21**) at a concentration of 4 μM. The medium was removed, and the adherent cells were trypsinized. The cells were pelleted by centrifugation at 400*g* for 5 min and further resuspended in 1 mL of rhodamine 123 (10 μg/mL) for 30 min at room temperature and washed with PBS twice and resuspended in PBS. The samples were analyzed for fluorescence (FL-1 detector, filter 530/30 nm bandpass) by using the WinMDI software for flow cytometry.

Annexin V and PI Binding Assay. To assess the simultaneous observation of early phase of apoptotic and necrotic features, A2058 cells were treated with graded concentration of hybrid **21** for 24 h, and then cells were measured by cytometry by adding annexin V−FITC to 10^6 cells per sample according to the manufacturer's specifications (Bender MedSystems, Vienna, Austria). Simultaneously, the cells were stained with PI. Flow cytometry data were analyzed by the WinMDI software.

Acknowledgment. We would like to thank the National Science Council of the Republic of China for financial support.

Supporting Information Available: Spectra and HPLC data for target compounds **17**−**21**. This material is available free of charge via the Internet at http://pubs.acs.org.

References

(1) Thurston, D. E. Advances in the Study of Pyrrolo[2,1-*c*][1, 4]-benzodiazepine (PBD) Antitumor Antibiotics. In *Molecular Aspects of Anticancer Drug−DNA Interactions*; Neidle, S., Waring, M. J., Eds.; Macmillan Press: New York, 1993; Vol. 1, pp 54−88.

(2) Kohn, K. W. Anthramycin. In *Antibiotics III Mechanism of Action of Antimicrobial and Antitumor Agents*; Corcoran, J. W., Hahn, F. E., Eds.; Springer-Verlag: New York, 1975; pp 3−11.

(3) Hurley, L. H.; Petrusek, R. L. Proposed Structure of the Anthramycin-DNA Adduct. *Nature* **1979**, *282*, 529−531.

(4) Thurston, D. E.; Bose, D. S. Synthesis of DNA-Interactive Pyrrolo-[2,1-*c*][1, 4]benzodiazepines. *Chem. Rev.* **1994**, *94*, 433.

(5) Kyowa Hakko Kogyo Co., Ltd. Japanese Patent 58180487, 21 Oct 1983, Appl. 82-63630, 16 April 1982; 9 pp; *Chem. Abstr.* **1984**, *100*, 173150.

(6) Hu, W. P.; Wang, J. J.; Lin, F. L.; Lin, Y. C.; Lin, S. R.; Hsu, M. H. An Efficient Synthesis of Pyrrolo[2,1-*c*][1,4]benzodiazepine. Synthesis of the Antibiotic DC-81. *J. Org. Chem.* **2001**, *66*, 2881−2883.

(7) Cargill, C.; Bachmann, E.; Zbinden, G. effects of Daunomycin and anthramycin on Electrocardiogram and Mitochondrial Metabolism of the Rat Heart. *J. Natl. Cancer Inst.* **1974**, *53*, 481−486.

(8) Bose, D. S.; Thompson, A. S.; Chin, J.; Hartley, J. A.; Berardini, M. D.; Jenkins, T. C.; Neidle, S.; Hurley, L. H.; Thurston, D. E. Rational Design of a Highly Efficient Irreversible DNA Interstrand Cross-Linking agent Based on the Pyrrolobenzodiazepine Ring System. *J. Am. Chem. Soc.* **1992**, *114*, 4939−4941.

(9) Gregson, S. T.; Howard, P. W.; Hartley, J. A.; Brooks, N. A.; Adams, L. J.; Jenkins, T. C.; Kelland, L. R. Thurston, D. E. Design, Synthesis, and Evaluation of a Novel Pyrrolobenzodiazepine DNA-Interactive Agent with Highly Efficient Cross-Linking Ability and Potent Cytotoxity. *J. Med. Chem.* **2001**, *44*, 737−748.

(10) Gregson, S. T.; Howard, P. W.; Gullick, D. R.; Hamaguchi, A.; Corcoran, K. E.; Brooks, N. A.; Hartley, J. A.; Jenkins, T. C.; Patel, S.; Guille, M. J.; Thurston, D. E. Linker Length Modulates DNA Cross-Linking Reactivity and Cytotoxic Potency of C8/C8′ Ether-Linked C2-exo-Unsaturated Pyrrolo[2,1-c][1,4]benzodiazepine (PBD) Dimer. *J. Med. Chem.* **2004**, *47*, 1161−1174.

(11) Kamal, A.; Babu, A. H.; Ramana, A. V.; Ramana, K. V.; Bharathi, E. V.; Kumar, M. S. Design, Synthesis of Pyrrolo[2, 1-*c*][1, 4]benzodiazepines and Their Conjugates by Azido Reductive Cyclization Strategy as Potential DNA-binding Agents. *Bioorg., Med. Chem. Lett.* **2005**, *15*, 2621−2623.

(12) Kumar, R.; Lown, J. W. Design, Synthesis and in vitro Cytotoxic Studies of Novel Bis-pyrrolo[2,1-*c*][1,4]benzodiazepine-pyrrole and Imidazole Polyamide Conjugates. *Euro. J. Med. Chem.* **2005**, *40*, 641−645.

(13) Damayanthi, Y.; Reddy, B. S. P.; Lown, J. W. Design and Synthesis of Novel Bis-pyrrolo[2,1-*c*][1,4]benzodiazepine-Lexitrosin Conjugates. *J. Org. Chem.* **1999**, *64*, 290−292.

(14) Wang, J. J.; Hill, G. C.; Hurley, L. H. Template-directed Design of a DNA-DNA Crosslinker Based upon a Bis-tomaymycin-duplex Adduct. *J. Med. Chem.* **1992**, *35*, 2995−3002.

(15) Mountzouris, J. A.; Wang, J. J.; Thurston, D. E.; Hurley, L. H. Comparison of a DSB-120 DNA Interstrand Cross-Linked Adduct with the Corresponding Bis-tomaymycin Adduct: An Example of a Successful Template-Directed Approach to Drug Design Based upon the Monoalkylating Compound Tomaymycin. *J. Med. Chem.* **1994**, *37*, 3132−3140.

(16) (a) Hanka, L. J.; Dietz, A.; Gerpheide, S. A.; Kuentzel, S. L.; Martin, D. G. CC-1065 (NSC 298223) a New Antitumor Antibiotic. Production, In Vitro Biological Activity, Microbiological Assays and Taxonomy of the Producing Microorganism. *J. antibiot.* **1978**, *31*, 1211−11217. (b) Chidester, C. G.; Krueger, W. C.; Mizsak, S. A.; Duchamp, D. J.; Martin, D. G. The structure of CC-1065, a Potent Antitumor Agent, and its Binding to DNA. *J. Am. Chem. Soc.* **1981**, *103*, 7629−7635.

(17) Mitchell, M. A.; Kelly, R. C.; Wicnienski, N. A.; Hatzenbuhler, N. T.; Williams, M. G.; Petzold, G. L.; Slightom, J. L.; Siemieniak, D. R. Synthesis and DNA Crosslinking by a Rigid CPI Dimer. *J. Am. Chem. Soc.* **1991**, *113*, 8994−8995.

(18) Zhou, Q.; Duan, W.; Simmons, D.; Shayo, Y.; Raymond, M. A.; Dorr, R. T.; Hurley, L. H. Design and Synthesis of a Novel DNA-DNA Interstrand Adenine-Guanine Cross-Linking Agent. *J. Am. Chem, Soc.* **2001**, *123*, 4865−4866.

(19) Kase, H.; Iwahashi, K.; Matsuda, Y. K-252a, a Potent Inhibitor of Protein Kinase C from Microbial Origin. *J. Antibiot.* **1986**, *39*, 1059−1065.

(20) Akinaga, S.; Nomura,; Gomi, K.; Okabe, M. Diverse Effects of Indolocarbazole Compounds on the Cell Cycle Progression of Ras-transformed Rat Fibroblast Cells. *J. antibiot.* **1993**, *46*, 1767−1771.

(21) Wang, J. J. U.S. Patent 6939869 B2, Sep 6, 2005, Appl. 10/242802, Sep 12, 2002.

(22) Herlyn, M.; Clark, W. H.; Rodeck, U. Biology of Tumor Progression in Human Melanocytes. *Lab. Invest.* **1987**, *56*, 461−474.

(23) Meikrantz, W.; Schlegel, R. Apoptosis and the Cell Cycle. *J. Cell Biochem.* **1995**, *58*, 160−174.

(24) Wilson, M. R. Apoptosis: Unmasking the Executioner. *Cell Death Diff.* **1998**, *5*, 646−652.

(25) Johnson, L. V.; Walsh, M. L.; Chen, L. B. Localization of Mitochondria in Living Cells with Rhodamine 123. *Proc. Natl. Acad. Sci. U.S.A.* **1980**, *77*, 990−994.

(26) Johnson, L. V.; Walsh, M. L.; Bockus, B. J.; Chen, L. B. Monitoring of Relative Mitochondrial Membrane Potential in Living Cells by Fluorescence Microscopy. *J. Cell Biol.* **1981**, *88*, 526−535.

(27) Wang, J. J. U.S. Patent 6660856 B2, Dec 9, 2003, Appl. 10094140, Mar 8, 2002.

(28) Scudiero, D. A.; Shoemaker, R. H.; Paull, K. D.; Monks, A.; Tierney, S.; Nofziger, T. H.; Currens, M. J.; Seniff, D. D.; Boyd, M. R. Evaluation of a Soluble Tetrazolium/formazan Assay for Cell Growth and Drug Sensitivity in Culture Using Human and Other Tumor Cell Lines. *Cancer Res.* **1988**, *48*, 4827−4833.

(29) Plowman, J.; Dykes, D. J.; Hollingshead, M.; Simpson-Herren, L.; Alley, M. C. Human Tumor Xenograft Models in NCI Drug Development. In *Anticancer Drug Development guide: Preclinical Screening, Clinical Trials, and Approval;* Teicher, B., Ed. Humana Press: Totowa, NJ, 1997; pp 101−125.

(30) Puvvada, M. S.; Hartley, J. A.; Jenkins, T. C.; Thurston, D. E. A Quantitative Assay to Measure the Relative DNA-binding Affinity of Pyrrolo[2,1-*c*][1, 4]benzodiazepine (PBD) Antitumour Antibiotics Based on the Inhibition of Restriction Endonuclease Bam*HI*. *Nucleic Acids Res.* **1993**, *21*, 3671−3675.

(31) Thurston, D. E.; Morris, S. J.; Hartley, J. A. Synthesis of a Novel GC−Specific Covalent-binding DNA Affinity-cleavage Agent Based on Pyrrolobenzodiazepines (PBDs). *Chem. Commun.* **1996**, 563−565.

(32) Baraldi, P. G.; Balboni, G.; Cacciari, B.; Guiotto, A.; Manfredini, S.; Romagnoli, R.; Spalluto, G.; Thurston, D. E.; Howard, P. W.; Bianchi, N.; Rutigliano, C.; Mischiati, C.; Gambari, R. Synthesis, in Vitro Antiproliferative Activity, and DNA-Binding Properties of Hybrid Molecules Containing Pyrrolo[2,1-c][1,4]benzodiazepine and Minor-Groove-Binding Oligopyrrole Carriers. *J. Med Chem.* **1999**, *42*, 5131−5141.

(33) Scaduto, R. C.; Grotyohann, L. W. Measurement of Mitochondrial Membrane Potential Using Fluorescent Rhodamine Derivatives. *Biophys. J.* **1999**, *76*, 469−477.

(34) Kroemer, G.; Dallaporta, B.; Resche-Rigon, M. The Mitochondrial Death/life Regulator in Apoptosis and Necrosis. *Annu. Rev. Physiol.* **1998**, *60*, 619−642.

(35) Pervaiz, S.; Seyed, M.; Hirpara, J.; Clement, M.; Loh, K. Purified Photoproducts of Merocyanine 540 Trigger Cytochrome C Release and Caspase 8-Dependent Apoptosis in Human Leukemia and Melanoma Cells. *Blood* **1999**, *93*, 4096−4108.

(36) Weiner, S. J.; Kollman, P. A.; Case, D. A.; Singh, U. C.; Ghio, C.; Alagona, G.; Profeta, S.; Weiner, P., Jr. A New Force Field for Molecular Mechanical Simulation of Nucleic Acids and Proteins. *J. Am. Chem. Soc.* **1984**, *106*, 765−784.

JM050956Q